

Available online at www.sciencedirect.com

ScienceDirect

journal homepage: www.journals.elsevier.com/oceanologia

ORIGINAL RESEARCH ARTICLE

Steric and atmospheric contributions to interannual sea level variability in the eastern mediterranean sea over 1993–2019

Bayoumy Mohamed^{a,b,*}, Nikolaos Skliris^c

^aUniversity of Alexandria, Faculty of Science, Department of Oceanography, Alexandria, Egypt

^bDepartment of Arctic Geophysics, University Centre in Svalbard, Longyearbyen, Norway

^cOcean and Earth Science, University of Southampton, Southampton, United Kingdom

Received 21 April 2021; accepted 15 September 2021

Available online 1 October 2021

KEYWORDS

Sea level variability and trend;
Thermosteric and halosteric effect;
Atmospheric contribution;
Eastern Mediterranean

Abstract Sea level trends and their forcing over the eastern Mediterranean basin are investigated by using 27 years (1993–2019) of gridded sea level anomalies (SLA) derived from satellite altimetry and 9 tide gauge stations, along with sea surface temperature (SST) and temperature and salinity profiles. The contributions of atmospheric (wind and pressure) and steric components to the interannual variability of total SLA were evaluated. The thermosteric component represents the major contributor to the linear trend and was positive over most of the eastern Mediterranean, with a spatially averaged trend of 2.13 ± 0.41 mm/year, accounting for 69% of the total sea level trend (3.1 ± 0.61 mm/year). In contrast, the halosteric effect has a negative contribution to the steric SLA, with a mean trend of -0.75 ± 0.19 mm/year. The atmospheric component trend was much lower at 0.32 ± 0.24 mm/year. The interannual variability of SLA accounts for about 36% of overall sea level variability. Steric and atmospheric contributions to the interannual variability of sea level in the eastern Mediterranean account for about 52% and 18%, respectively. The strongest interannual variability and trends in SLA were observed over the basin's main recurrent gyres, with the maximum positive trend obtained over the Mersa–Matruh and Cyprus gyres, as well as the North Shikmona eddy, and maximum negative trend over the Ierapetra gyre. Over the study period, all tide gauges showed a positive and statistically significant trend, ranging from 1.47 ± 0.77 to 5.79 ± 1.32 mm/year after applying glacial isostatic

* Corresponding author at: University of Alexandria, Faculty of Science, Department of Oceanography, Alexandria, Egypt.

E-mail addresses: m.bayoumy@alexu.edu.eg, mohamedb@unis.no (B. Mohamed).

Peer review under the responsibility of the Institute of Oceanology of the Polish Academy of Sciences.



<https://doi.org/10.1016/j.oceano.2021.09.001>

0078-3234/© 2021 Institute of Oceanology of the Polish Academy of Sciences. Production and hosting by Elsevier B.V. This is an open access article under the CC BY-NC-ND license (<http://creativecommons.org/licenses/by-nc-nd/4.0/>).

adjustment and atmospheric correction, and were in good agreement with reconstructed steric sea level data.

© 2021 Institute of Oceanology of the Polish Academy of Sciences. Production and hosting by Elsevier B.V. This is an open access article under the CC BY-NC-ND license (<http://creativecommons.org/licenses/by-nc-nd/4.0/>).

1. Introduction

Quantifying sea level change and assessing its main forcing mechanisms have recently been at the forefront of challenges for the climate research community. The Mediterranean Sea has been identified as one of the most vulnerable regions to climate change (Giorgi, 2006). In particular sea level rise may have a strong impact in the Eastern Mediterranean (EM) Sea due to the many low-lying densely populated coastal areas such as the Nile River Delta in Egypt (Church et al., 2013). Sea level rise may strongly affect livelihoods in coastal populations and various essential economic activities of the countries surrounding the Eastern Mediterranean Sea including fishing, tourism, irrigation, transportation, and more recently, natural gas drilling projects.

Generally, the global mean sea level change depends on both mass addition (including glacier ice melting and changes in ground water storage) and redistribution, as well as on the steric effect, which is caused by changes in water-column density due to temperature and salinity variations (Ishii and Kimoto, 2009; Jordà and Gomis, 2013; Levitus et al., 2012). Since the rate of global sea-level rise is not uniform, and it is highly dependent on location (Stammer et al., 2013), studies of regional sea level variations and physical processes controlling them are required. Here, our study focuses on sea level change and its contributing mechanisms in the eastern Mediterranean Sea.

During the altimetry era, extensive work has been conducted to measure sea level variability and trends in the Mediterranean Sea. Mohamed et al. (2019a) revealed a strong positive sea level trend of 2.7 ± 0.41 mm/year (after glacial isostatic adjustment correction), as well as a substantial warming of $0.036 \pm 0.003^\circ\text{C}/\text{year}$ over the whole Mediterranean over 1993–2017. Bonaduce et al. (2016) reported that the Mediterranean Sea level has strongly risen with an average trend of 2.44 ± 0.5 mm/year over 1993–2012. However, spatial variability of the trend was quite large with the eastern basin showing much higher trends as compared with the western basin, whereas even negative trends were observed in large parts of the Ionian Sea. The Mediterranean Sea upper-layer heat and salt contents are modulated at interannual/decadal timescales by the natural climate variability modes of the North Atlantic (Tsimplis and Josey, 2001), especially the North Atlantic Oscillation (NAO) (Hurrell, 1995), strongly affecting thermosteric sea level variability (Landerer and Volkov, 2013; Tsimplis et al., 2013). Previous studies have demonstrated that SST and SLA are highly correlated at seasonal and interannual scales, especially in the eastern Mediterranean basin (Cazenave et al., 2002; Fenoglio-

Marc, 2002). The strong correlation between the two parameters suggests that the thermosteric effect is a major factor controlling interannual variability of sea level in the eastern Mediterranean (Vigo et al., 2005). In general SLA interannual variability is more pronounced in the Eastern Mediterranean as compared with the western basin (Bonaduce et al., 2016; Cazenave et al., 2002). The eastern Mediterranean was strongly affected by the rapid rise in sea level over 1993–2001 with rates of 5–10 mm/year, which was partially attributed to accelerating sea surface warming (Cazenave et al., 2001; Vigo et al., 2005). Tsimplis et al. (2005) also associated the increasing sea level rise during that period to the Eastern Mediterranean Transient (Roether et al., 1996), a major climatic transient event during the 1990's affecting the EM thermohaline closed cell with the main source of deep water shifting from the Adriatic to the Aegean Sea. Roether et al. (1996) showed that an exceptionally dense Aegean Sea outflow had replaced 20% of the EM deep waters by the mid-nineties, lifting the older deep water of Adriatic origin and resulting in large changes of the EM overturning circulation and salt content distribution. More recently, Banaduce et al. (2016) found that the Mediterranean SLA trend over 1993–2012 was partially driven by strong positive SLA anomalies in 2010 and 2011 that mainly occurred in the eastern basin.

The role of atmospheric forcing in determining sea level variability and trends in the Mediterranean is well demonstrated by several studies (Gomis et al., 2008; Marcos and Tsimplis, 2008; Tsimplis et al., 2005). Considering dynamic atmospheric correction (DAC), Pascual et al. (2008) observed a sea level trend of about 0.6 mm/year over the period 1993–2001 due to the atmospheric forcing. The same authors observed minimum values in the western Mediterranean basin and maximum values in the Levantine basin up to 2 mm/year.

The main objective of this study is to investigate the interannual variability and trends of total SLA and its contributors in the eastern Mediterranean, based on altimetry and tide gauge sea level anomalies, as well as high resolution 3-D temperature and salinity observations from 1993 to 2019. In particular, we estimate the relative contributions of atmospheric, Glacial Isostatic Adjustment (GIA), thermosteric, halosteric, and total steric effects to SLA variability and trends.

2. Data and methodology

The contributions of the atmospheric and steric effects to the interannual sea level variability in the eastern Mediterranean Sea were analyzed using different data sources, as described in the following sub-sections.

Table 1 Sea level trends (mm/year) for the observed tide gauges (TG), atmospheric, total steric and residual (observation minus atmospheric, GIA, and total steric) contributions to the sea level trend. R denotes the correlation coefficients between the atmospherically corrected TG and reconstructed steric sea level. All uncertainties are given at the 95% confidence interval. Not statistically significant trends are underlined in boldface.

Stations (Country)	Period	Trend (mm/year)						R
		TG	GIA	DAC	TG*	Steric	Residual	
Siros (Greece)	1993–2019	3.21±0.83	0.09	0.54±0.31	2.66±0.64	1.18±0.42	1.65±0.57	0.70
Khalkis north (Greece)	1993–2019	3.98±0.84	-0.05	0.58±0.36	3.46±0.61	1.83±0.41	1.61±0.63	0.64
Thessaloniki (Greece)	1993–2019	4.46±0.96	-0.17	0.60±0.38	3.78±0.70	1.17±0.28	2.84±0.63	0.73
Alexandroupolis (Greece)	1993–2019	1.95±1.03	-0.12	0.50±0.36	1.47±0.77	1.30±0.30	0.23±0.67	0.53
Khios (Greece)	1993–2013	3.02±1.37	-0.04	0.51±0.31	1.57±0.66	0.82±0.38	0.11±1.02	0.78
Leros (Greece)	1993–2019	2.00±0.80	0.03	0.40±0.27	2.00±0.80	1.27±0.37	2.00±0.80	0.47
Antalya II (Turkey)	1993–2009	6.48±1.48	-0.09	0.59±0.23	5.79±1.32	1.36±0.40	4.42±1.20	0.69
Hadera (Israel)	1993–2019	4.18±0.77	0.02	0.17±0.17	4.03±0.69	1.30±0.38	2.82±0.63	0.73
Alexandria (Egypt)	1993–2015	5.01±0.94	-0.01	0.21±0.22	4.65±0.88	2.00±0.41	1.85±0.92	0.73

* Indicates that GIA, and DAC correction was applied to TG.

2.1. Altimetry and tide gauge mean sea level data

Monthly mean sea level data from 9 tide gauges (TG) stations (Table 1) obtained from the Permanent Service for Mean Sea Level (PSMSL) (Woodworth and Player, 2003) (<http://www.psmsl.org/>, accessed December 2020) were used in this study. The spatial distribution of these tide gauges stations over the eastern Mediterranean Sea is represented by black triangles, as shown in Figure 1. All stations have datum continuity and data exceeding 15 years. At the Alexandria station, a datum correction was applied as we extended the PSMSL record by 10 years of monthly data (2006 to 2015), which was quality controlled by Mohamed et al. (2019b).

Gridded daily mean sea level anomalies (SLA) at 1/8-degree spatial resolution for the period 1993–2019 were obtained from the Copernicus Marine Environment Monitoring Service (CMEMS; <http://marine.copernicus.eu/>, accessed December 2020). Monthly means were calculated from the daily values at each grid point. The data are produced by merging observations of T/P, ERS1/2, Jason 1/2/3, Sentinel-3A, HY-2A, Saral/AltiKa, Cryosat-2, ENVISAT, and GFO altimetry missions. This dataset is distributed under the name SEALEVEL_MED_PHY_L4_REP_OBSERVATIONS_008_051 in the CMEMS catalogue. In which, all standard geophysical and environmental corrections have been applied, including atmospheric correction using the so-called dynamic atmospheric correction (DAC) (Landerer and Volkov, 2013; Pujol and Larnicol, 2005), which combines the low frequencies (>20 days) of the standard inverted barometer (IB) correction with the outputs of the barotropic MOG2D-G model (Carrère and Lyard, 2003). This procedure improves the representation of high-frequency (<20 day) atmospheric forcing considering both pressure and wind effects.

2.2. Atmospherically induced sea level variations

Dynamic atmospheric corrections were applied by AVISO processing algorithms to correct satellite altimetry data. Here, we analyze the DAC product to estimate the contribution of atmospheric forcing to the satellite altimetry and to correct TG data. This data is provided by AVISO website

(<ftp.aviso.altimetry.fr>, accessed December 2020) as an auxiliary dataset with a spatial grid resolution of $0.25^\circ \times 0.25^\circ$ and a time resolution of 6 hours. The data were converted to monthly means to be consistent with altimetry and TG data used in this study.

2.3. Estimation of steric, thermosteric, and halosteric sea level anomalies

Steric SLA (SSLA) was calculated as the vertical integral of the density anomaly and then decomposed into thermosteric SLA (TSLA), and halosteric SLA (HSLA) by using the following equations (Jayne et al., 2003; Wang et al., 2017):

$$\begin{aligned} \text{SSLA} &= \text{TSLA} + \text{HSLA} = \frac{-1}{\rho_0} \int_{-H}^0 \Delta\rho \, dz \\ &= - \int_{-H}^0 (\alpha\Delta T - \beta\Delta S) dz \end{aligned}$$

Where ρ_0 is the reference density (1025 kg/m^3), z denotes depth. And $\Delta\rho$, ΔT , and ΔS are density, temperature, and salinity anomalies, respectively, referred to their climatic mean (1993–2019) at each layer, and α and β are the thermal expansion and saline contraction coefficient, respectively, calculated from monthly temperature and salinity using the Thermodynamic Equation Of Seawater-2010 (TEOS-10) (Pawlowicz et al., 2012), and the Gibbs Sea Water (GSW) Oceanographic Toolbox (McDougall and Barker, 2011). H is the reference depth, which is set to 400 m or the bottom where the sea is shallower. The choice of 400 m for the lower level of integration was made here to be consistent with Tsimplis and Rixen, (2002). The steric effect in the Mediterranean Sea is limited to the upper 300 m of the water column, as shown by Tsimplis et al. (2013).

The steric height and its components were calculated using a high resolution monthly 3-D hydrographic gridded product provided by CMEMS (MULTIOBS_GLO_PHY_TSUV_3D_MYNRT_015_012, <https://www.copernicus.eu/en>, accessed January 2021). This dataset is based on optimal interpolation of global quality-controlled ocean temperature and salinity profiles (Guinehut et al., 2012). It has a horizontal resolution of $0.25^\circ \times 0.25^\circ$ and

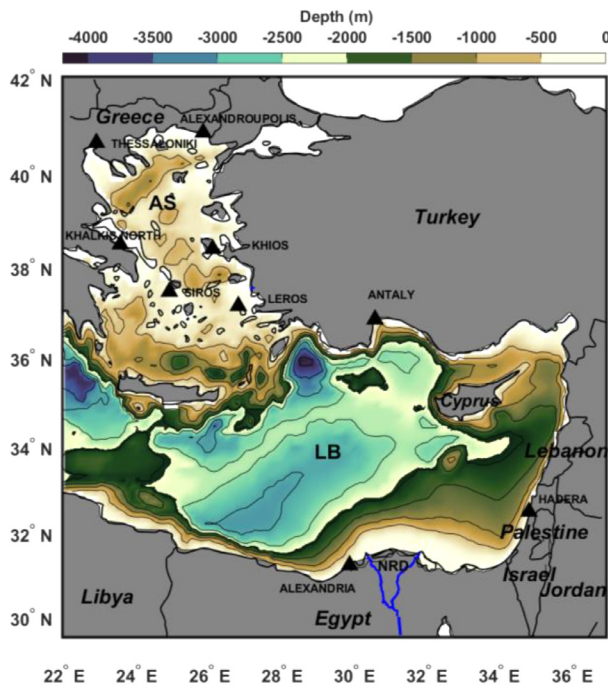


Figure 1 Bathymetry of the study area and the location of the tide gauges used in our study (black triangles). Bathymetric data obtained from a global 30 arc-second interval grid (GEBCO, <https://www.gebco.net>) with 10 m as the minimum depth. The abbreviations stand for the Levantine Basin (LB), the Aegean Sea (AS), and the Nile River Delta (NRD).

a vertical resolution of 50 depth levels (standard depths) covering the period 1993–2019.

In addition, in order to investigate SST variations we use the NOAA Daily Optimum Interpolation Sea Surface Temperature dataset (version 2.1, NOAA_DOISST_V2.1, <https://www.ncei.noaa.gov/data/sea-surface-temperature-optimum-interpolation/v2.1/access/avhrr/>, accessed January 2021), with a spatial resolution of $0.25^\circ \times 0.25^\circ$, covering the period 1993–2019 (Huang et al., 2021). The ICE-6G_C (VM5a) model provided by PSMSL (Peltier et al., 2015) is used for the GIA correction. The rate of relative sea level rise (dSea) and rate of change of geoid height (dGeoid) in this model (Peltier et al., 2015) are used to correct tide gauge and altimetry data used in our study, respectively.

2.4. Linear trends of sea level and its components

Linear trends of the observed, atmospherically induced, steric, and residual (observation minus atmospheric, GIA, and total steric) sea level as well as SST over the period 1993–2019 are estimated by using the least squares method (Wilks, 2011). To properly estimate long-term trends and assess interannual and interdecadal variability of sea level it is important to remove the strong effect of seasonal variability. Thus, the mean and seasonal cycles were removed from the all-time series prior to the trend calculation. A 12-month climatology is built for each time series by averaging the monthly mean values for each calendar month at each grid point from 1993 to 2019. Then, the de-seasoned anomaly field is obtained by subtracting the

monthly climatology from each dataset. Since the Eastern Mediterranean is an eddy-rich area with eddies strongly affecting intra-annual variability, a 13-month running mean was used to highlight interannual variability. These trends were tested for statistical significance using the original two-tailed modified Mann-Kendall test at the 95% confidence interval (Hamed and Ramachandra Rao, 1998). MATLAB software R2020b, and Climate Data Toolbox (CDT) are used to estimate trends, remove seasonal cycles, and apply the Mann-Kendall test (Greene et al., 2019).

3. Results and discussion

In this section, the spatial and temporal variability of the total sea level from altimetry and tide gauges is analyzed in detail over the period 1993–2019. Then relative contributions of the atmospheric, GIA and steric effects to total change in sea level are explored.

3.1. Observed mean sea level changes

A few TG stations are available in the eastern Mediterranean during the study period. Trends in sea level based on TG measurements and their estimated steric height are compared in Figure 2 and Table 1. The tide gauges time series show high coherence at all stations, suggesting that they are determined by large scale rather than local meteorological components. The total sea level trends are positive at all TG stations over the period 1993–2019, ranging from 1.95 ± 1.03 mm/year at Alexandroupolis (Greece) to 6.48 ± 1.48 mm/year at Antalya II (Turkey). The high trend at the Antalya II station is significantly affected by local land subsidence, which was about -3.2 ± 0.5 mm/year based on GPS data for the period 1994–2009 (Simav et al., 2012). Also, the vertical land motion was higher at Thessaloniki, Leros, and Hadera stations, as demonstrated by Fenoglio-Marc et al. (2004) and Mohamed and El-Din (2019).

Figure 3 depicts the spatial distribution of altimetry SLA trend and its components. The average spatial trend of the total atmospherically corrected SLA for the whole region is 3.1 ± 0.61 mm/year. The GIA correction to altimetry data (dGeoid) is negative in the whole region, with values ranging from about -0.1 to -0.18 mm/year. Figure 3a shows the trends in altimetry after the GIA effect is removed. On average, these are about 0.13 mm/year larger due to the GIA effect on altimetry data. The average altimetry trend for the eastern Mediterranean after GIA correction is about 3.23 ± 0.61 mm/year. The SLA trend is spatially coherent over most of the eastern Mediterranean where strong positive trends (up to 5.6 mm/year) were observed, while only the Ierapetra gyre (southeast of Crete) showed a significantly negative trend. The highest positive trend has been observed over the Mersa-Matruh and Cyprus gyres, as well as the North Shikmona eddy (Figure 3a). These gyres and eddies' positions are well defined by Menna et al. (2021). The general spatial pattern of SLA trend is in agreement with earlier studies (Bonaduce et al., 2016; Mohamed et al., 2019a; Taibi and Haddad, 2019). Relatively low (and not statistically significant at 95% confidence interval) trends were only found in the south-west part of the basin.

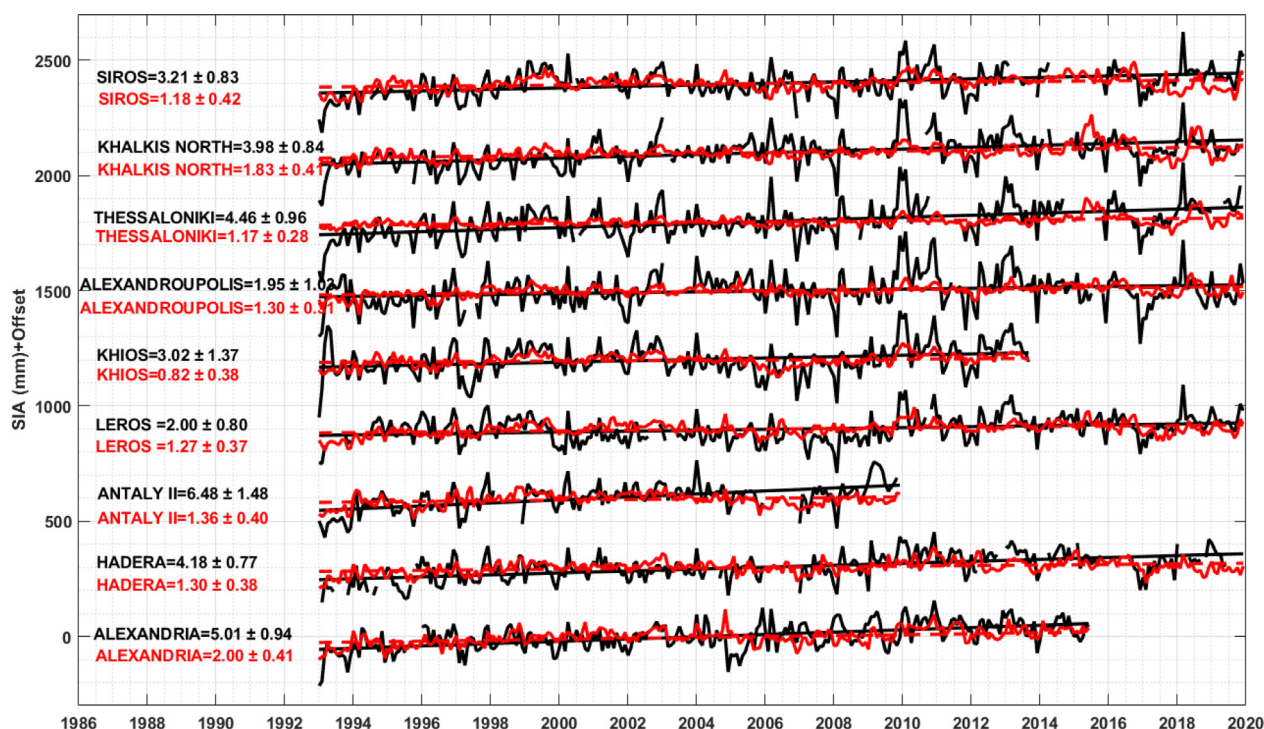


Figure 2 Comparison between observed tide gauge (black) and steric sea level (red) at the available tide gauge stations in the eastern Mediterranean Sea, the mean and seasonal cycles have been removed from all-time series.

Figure 4 shows the time evaluation of the mean sea level anomaly and its components in the Eastern Mediterranean from 1993 to 2019. The total atmospherically corrected SLA shows a positive trend of 3.05 ± 0.25 mm/year. The long-term trend has been found to be partially driven by the extreme positive anomaly occurred in 2010, which is mainly attributed to the strong negative phase of North Atlantic Oscillation (NAO) (Landerer and Volkov, 2013). Both the steric and mass (residual) component contribute positively to the total SLA trend. However, the mass component shows a higher variability and a stronger trend than the steric component (Figure 4a).

Separating the steric component into its thermosteric and halosteric contributions reveals that the rapid sea level rise is primarily due to the thermosteric component, while the halosteric contribution is negative, especially over the last 15 years (Figure 4b), indicating an increase in mean salinity over the entire domain (Figure 5d). The atmospheric contribution shows a slightly positive trend, as shown in Figure 4c. This result is consistent with (Gomis et al., 2008), who demonstrated that the atmospheric circulation pattern had changed dramatically in the Mediterranean Sea over the last decade, with a positive trend in the contribution of atmospheric pressure estimated from 1993 to 2001.

3.2. The atmospheric contribution

Over the analyzed period, the contribution of DAC at TG stations shows a positive trend (Table 1 column 5), with the highest trends found in the Aegean Basin, with a maximum value of about 0.60 ± 0.38 mm/year at Thessaloniki (Greece). The atmospheric contribution to sea level trend in the Levantine Basin is negligible, as evidenced by low and not significant DAC trends at Alexandria (Egypt) and

Hadera (Israel) stations. Figure 3b depicts the spatial distribution of trends in atmospheric pressure and wind components (DAC) from 1993 to 2019. The average spatial trend is 0.32 ± 0.24 mm/year, with values ranging from 0 to 0.72 mm/year. The eastern part of the EM shows the lowest (and not statistically significant) values, while the western part and the Aegean Sea shows the highest values. The DAC's average contribution accounted for about 10% of the overall sea level trend in EM.

3.3. SST, temperature, and salinity changes

The spatial distribution of the SST linear trends (Figure 5a) shows that significantly positive SST trends are observed throughout the entire basin. Stronger warming is obtained in the Levantine basin, with values up to $0.06^\circ\text{C}/\text{year}$ in the Cretan Arc and west and south of Cyprus, while much weaker warming ($\sim 0.01^\circ\text{C}/\text{year}$) is observed in the Ierapetra gyre, southeast of Crete. This spatial pattern is in good agreement with that reported by (Skliris et al., 2012) for the period 1992–2008 and with (Ibrahim et al., 2021) over the period 1982–2020. SST and sea level trend maps have similar spatial patterns, with strong sea surface warming coinciding with strong sea level rise and vice versa, except from the north part of the Aegean Sea. This correlation suggests that the thermosteric effect is the main factor controlling interannual sea level variability in the eastern Mediterranean.

Figures 5b and c show the averaged water-column (0–400 m depth) temperature and salinity trend maps, respectively. A strong positive and statistically significant trend in water-column averaged temperature was observed over most of the region following the accelerating surface warming of the Mediterranean Sea. An exception to this

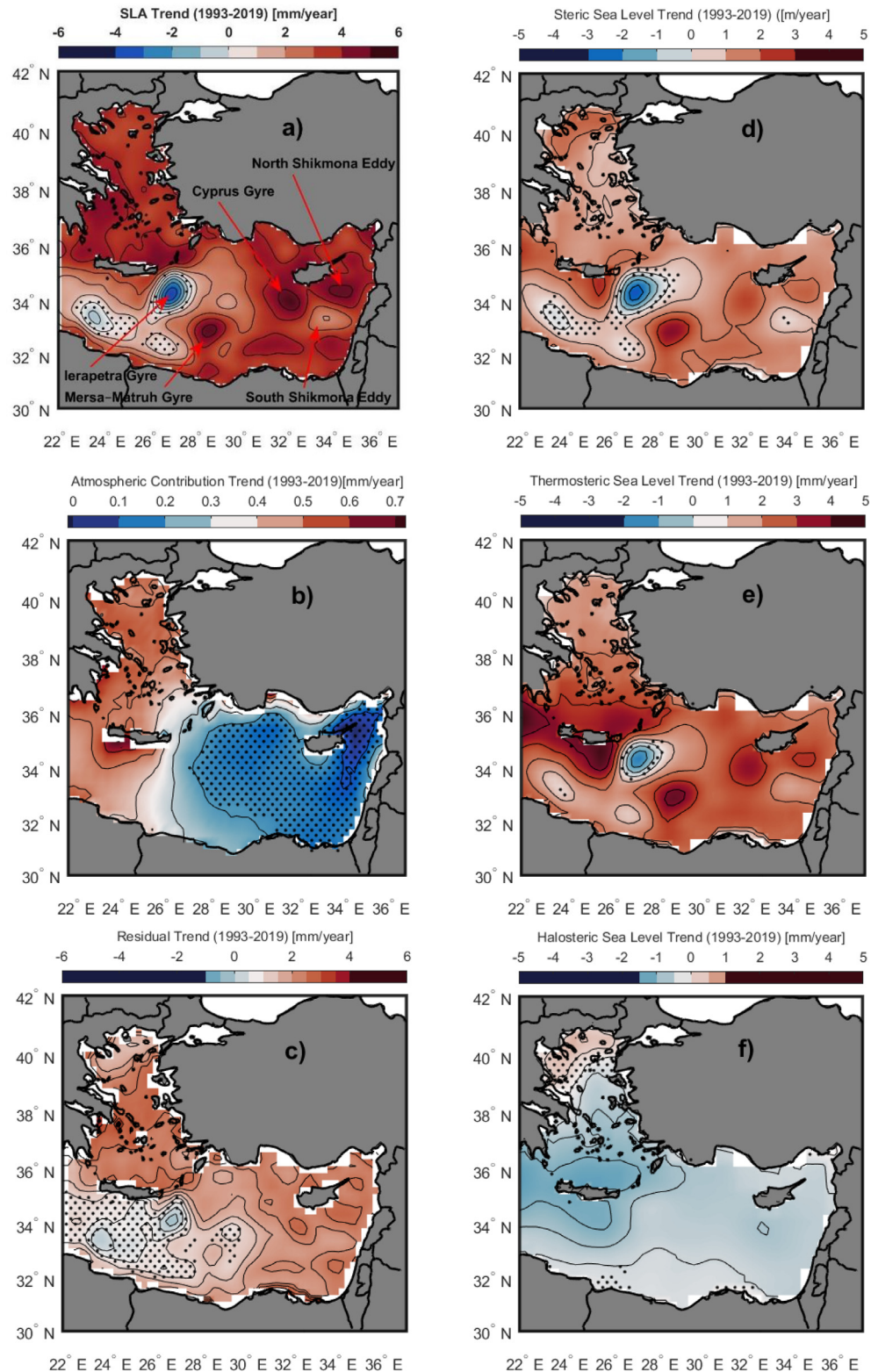


Figure 3 Spatial patterns of trends (mm/year) over the period 1993–2019 for (a) the total atmospherically corrected SLA from altimetry after the application of the GIA correction, (b) atmospheric contribution to sea level from DAC, (c) altimetry after the steric component and the GIA correction are removed (residual), and (d, e, and f) steric, thermosteric and halosteric components, respectively. Mean and seasonal cycles were removed from all-time series at each grid points. Regions where the trends are not statistically significant at the 95% confidence interval are stippled. Major gyres mentioned in the text are also depicted in Figure 3a.

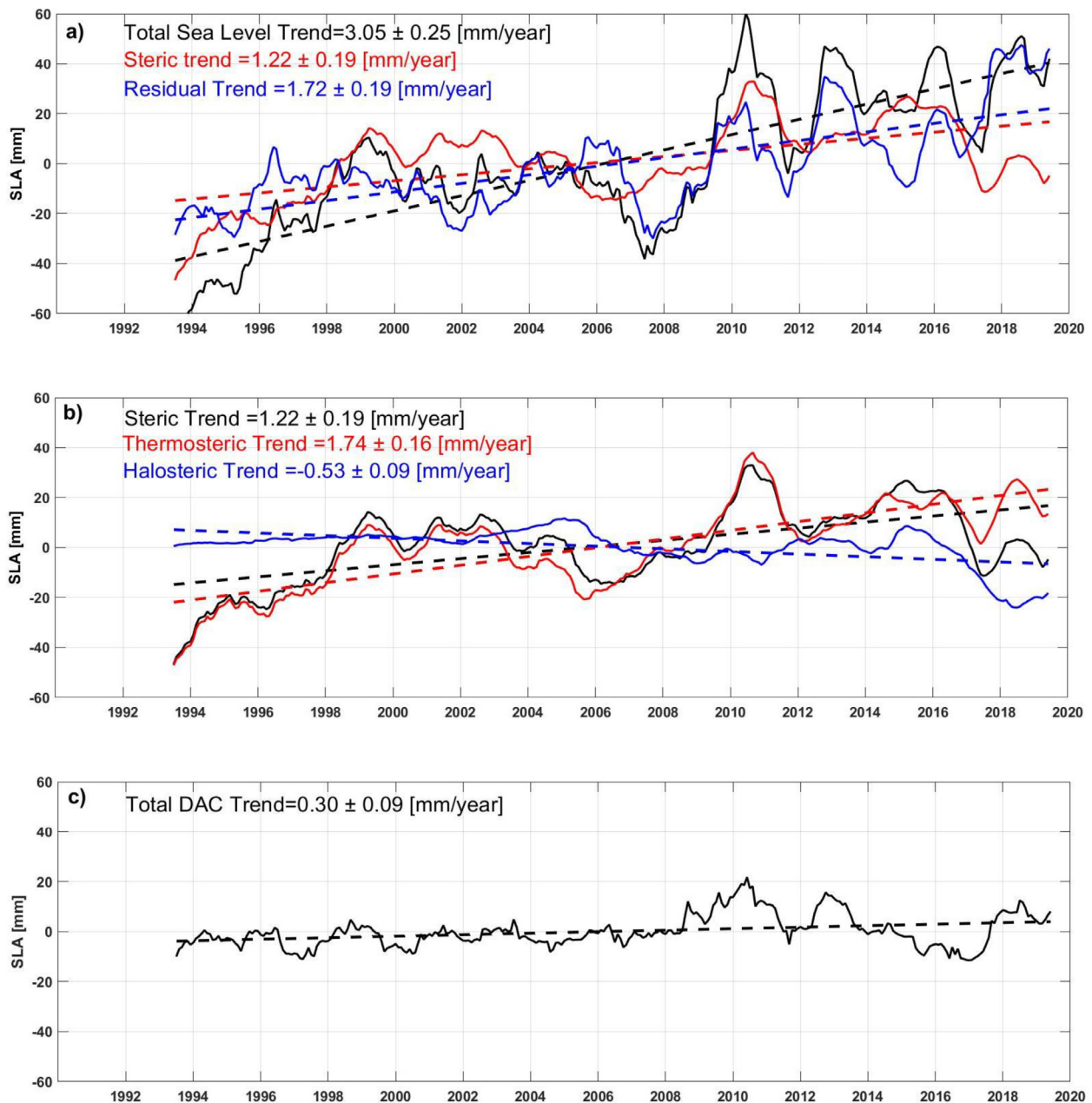


Figure 4 Time evaluation of the mean sea level anomaly and its components in the Eastern Mediterranean over 1993–2019. a) Total atmospherically corrected altimetry SLA, steric component computed from the CEMES dataset, and residual component (the difference between the total atmospherically corrected sea level and steric effect). b) The contributions of the thermosteric and halosteric components to the total steric effect. c) Dynamic atmospheric contribution to the total sea level. The de-seasoned monthly time series have been low passed for improved visualization by using a 13-month running mean.

widespread upper-layer heat content increase is the Ierapetra gyre, where a negative trend was found. Salinity has been found to be increasing over most of the region during the same period, with the strongest trends obtained in the South Aegean and northwest part of the Levantine Basin. An acceleration of salt content increase of the Eastern Mediterranean has been observed over the last few decades linked with strong net evaporation increase, coincident with acceleration of surface warming and subsequent increase of latent heat loss over the Mediterranean surface (Skliris et al., 2018).

In contrast with the widespread strong increase in the upper layer salt content of EM a low negative (and mostly not statistically significant) trend was observed along the Egyptian coast and the north part of the Aegean Sea. Upper layer salinity in both these regions is controlled by freshwater inputs (Nagy et al., 2017; Skliris et al., 2018), under the influence of the Nile River and the Black Sea outflows, respectively.

The de-seasoned spatial mean of the SST and the averaged water-column (0–400 m depth) temperature and salinity timeseries in the eastern Mediterranean Sea for

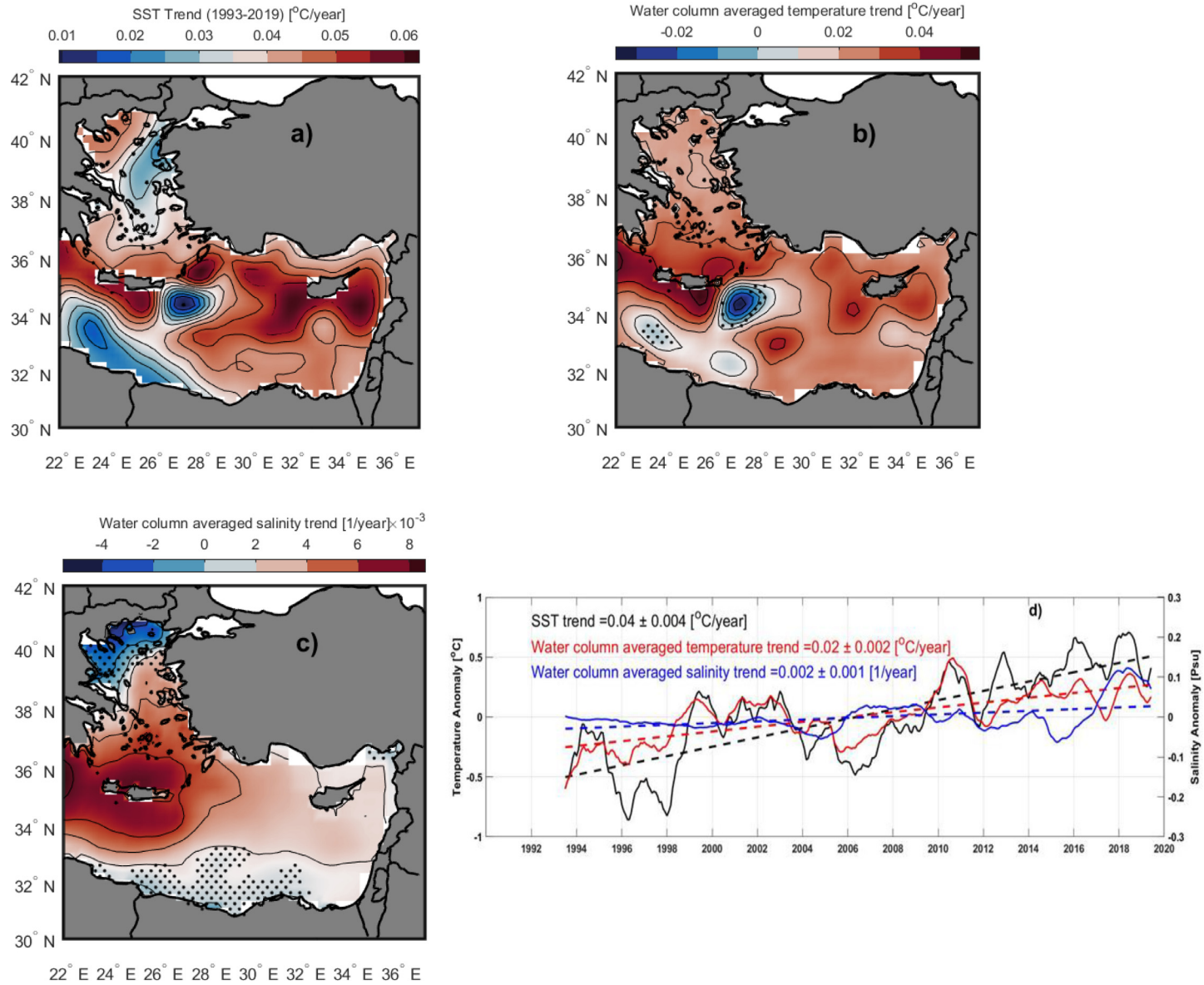


Figure 5 Spatial distribution of trends (mm/year) over the period 1993–2019 for: (a) SST, (b and c) averaged water column (from 0 to 400 m) temperature and salinity, respectively. (d) The de-seasoned monthly mean time series and linear trends for the averaged of SST (black), 3-D spatially averaged temperature (red) and salinity (blue) over the eastern Mediterranean basin. To enhance the visualization and to emphasize inter-annual variability, the data was low passed using a 13-month moving average. Regions where the trends are not statistically significant at the 95% confidence interval are stippled.

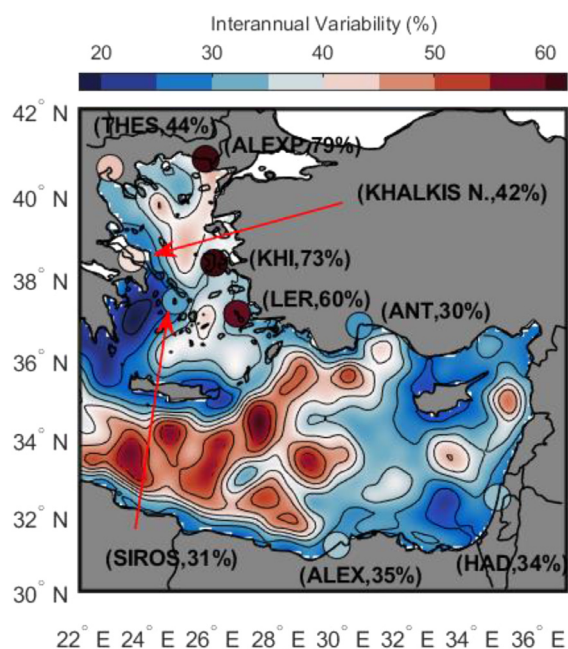


Figure 6 Percentage of the variance explained by the inter-annual variability of SLA from Altimetry (contour map) and tide gauges (circles). For each tide gauge station, the value of variance explained is also provided between brackets next to the station name.

the period 1993–2019 are shown in Figure 5d. The SST shows a positive trend of $0.04 \pm 0.004^\circ\text{C}/\text{year}$, which is consistent with (Pastor et al., 2020) for the 1982–2019 period over the eastern Mediterranean Sea. The spatial mean 0–400 m water-column temperature and salinity show positive statistically significant trends of $0.02 \pm 0.002^\circ\text{C}/\text{year}$, and $0.002 \pm 0.001 \text{ psu}/\text{year}$, respectively, over 1993–2019. Although inter-annual variability is important there seems to be an accelerating trend for both parameters following the increasing surface warming rate of the basin over the last 15 years.

3.4. The steric contribution

The steric contribution to sea level trends is positive at all TG stations (Table 1, column 7), with values ranging between $0.82 \pm 0.38 \text{ mm}/\text{year}$ at Khios station and $2.00 \pm 0.41 \text{ mm}/\text{year}$ at Alexandria station. The de-seasoned monthly time series of steric contribution closely follow but show much lower inter-annual variability compared to observed total sea level at all TG stations (Figure 2). However, there are some deviations from the observations, especially in the Aegean Sea stations, induced by other processes that are not resolved in our study. The strong positive anomaly in 2010 is mainly caused by the strong negative NAO event, as indicated by (Landerer and Volkov, 2013; Tsimplis et al., 2013). In general, there is a good correlation between observed and reconstructed steric sea level, with correlations up to 0.7, as shown in Table 1.

Figure 3d shows the spatial distribution of the steric sea level trends. Steric sea level shows a positive significant trend over the whole Basin, except from the Ierape-

tra gyre, where a negative trend of up to $-3.5 \text{ mm}/\text{year}$ was observed. The spatial distributions of the observed and estimated steric sea level trends are very similar (see, Figure 3a and d), which are largely explained by temperature variations with the difference being probably due to the mass contribution. The correlation coefficient between the observed SLA and steric height was 0.68 (statistically significant at the 95% confidence interval). The spatial average of steric trend over the entire basin was about $1.38 \pm 0.42 \text{ mm}/\text{year}$, which accounts for about 45% of the total sea level trend ($\sim 3.1 \text{ mm}/\text{year}$).

Figures 3e and f show the thermosteric and halosteric sea level trends maps, respectively. The thermosteric sea level trend patterns are similar to the steric sea level trend patterns (see, Figure 3d and e), demonstrating that the steric sea level in the EM is dominated by temperature changes. The correlation coefficient between the observed SLA and thermosteric height was 0.73 (statistically significant at the 95% confidence interval). The thermosteric expansion, which has a basin average of about $2.13 \pm 0.41 \text{ mm}/\text{year}$, is responsible for most of the steric trend and accounts for 69% of the total sea level trend. Most of the eastern Mediterranean Sea has negative halosteric trends, with a basin average of $-0.75 \pm 0.19 \text{ mm}/\text{year}$, except in the north part of the Aegean Sea, where a positive trend of up to $1 \text{ mm}/\text{year}$ was observed, possibly due to mixing with less saline water from the Black Sea (Stanev et al., 2000). The halosteric component contributes (negatively) by 24% to the total sea level trend.

3.5. Residuals contribution

The residual trends include the contribution of oceanic mass addition and local vertical land movement such as sediment load or compaction. Groundwater extraction and tectonics can also contribute to the residual trends of the tide gauge. The GIA values at all TG stations are very small, ranging from $-0.17 \text{ mm}/\text{year}$ at Thessaloniki (Greece) to $0.09 \text{ mm}/\text{year}$ at Siros (Greece). The residuals obtained after the GIA, atmospheric and total steric effects were removed from the observations, indicate positive trends which are statistically significant at all stations, except from Alexandroupolis and Khios stations in the North Aegean Sea.

The spatial distribution of the residual trend is shown in Figure 3c. The higher values were found in the Aegean Sea, while the lower values were observed in the Levantine basin, with an average value of $1.6 \pm 0.51 \text{ mm}/\text{year}$ over the entire basin. Results suggest that the mass component is the dominant contributor to sea level trend in the Aegean Sea, while the steric component is the dominant contributor in the Levantine Sea.

3.6. Inter-annual variability

To quantify the interannual variability of sea level, we calculate the basin-averages of temporal variances at each grid point for both the observed datasets, which represent total variability, and the residual datasets, which represent the de-seasoned and detrended signal (Torres and Tsimplis, 2013). We found that, on average, the inter-annual variability of sea level accounts for 36% of the total

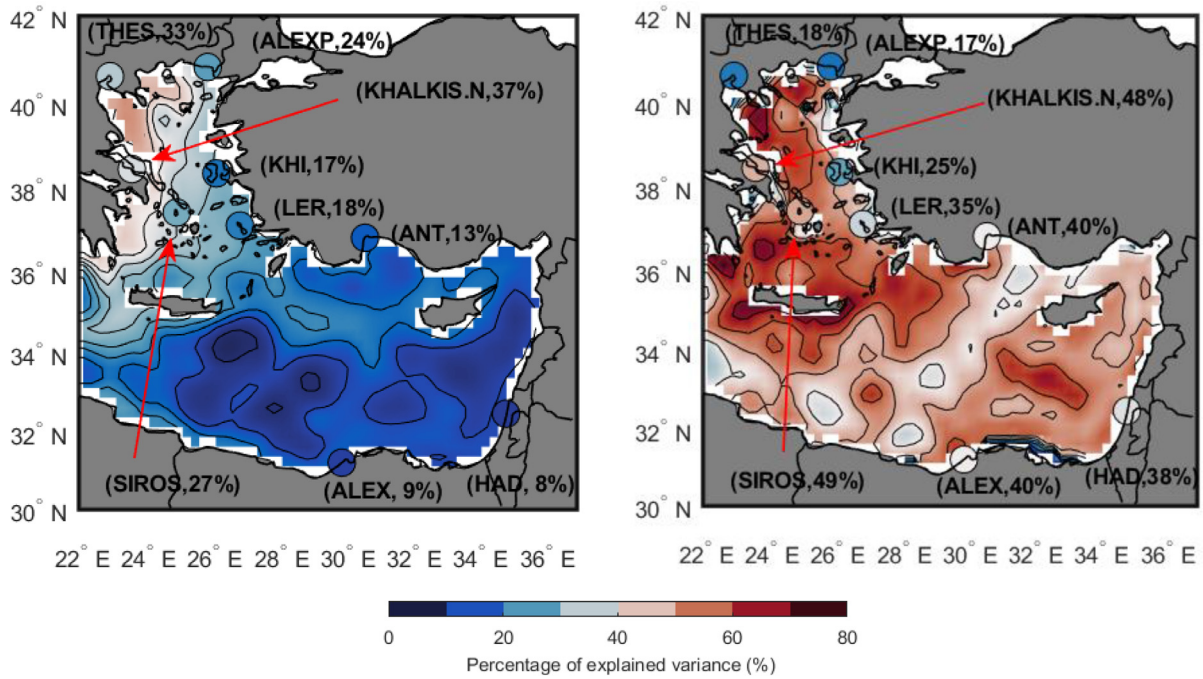


Figure 7 Percentage of SLA inter-annual variability explained by a) atmospheric contribution, and b) total steric height above 400 m over 1993–2019.

variability in the entire basin, with a range of 18 to 62% (Figure 6). Higher interannual variability has been observed over the major circulation features and recurrent gyres of the basin, with the maximum percentage of the explained variance was found over the southwest part of the Aegean Sea, with less than 25% of sea level variability explained. The same results were obtained from tide gauges, except for three TG stations (Leros, Khios, and Alexandroupolis) on the Aegean Sea’s eastern coast, which show greater interannual variability, probably due to the small variance of observed sea level variability in that region.

We also evaluated the contribution of atmospheric and steric sea level to the inter-annual variability of total SLA at regional scale as shown in Figure 7. The atmospheric effect explains from 3% to 50% of the variability, with a basin average of 18%. The percentage of variance explained by the atmospheric contribution is much larger in the Aegean Sea, peaking in the northwestern part of the basin. The steric component of the sea level explains more than 40% of SLA variability in most regions. On average, the steric component accounted for 52% of the interannual sea level variability. Therefore, the changes in atmospheric and steric components account for 70% of the interannual sea level variability in the Eastern Mediterranean.

4. Summary and conclusions

In this study, we have assessed the contribution of atmospheric, GIA, and steric components to the interannual variability and trend of sea level in the Eastern Mediter-

ranean Sea over the period 1993–2019, using altimetry and tide gauge SLA, together with hydrographic and atmospheric datasets.

After applying atmospheric and GIA correction, we found a spatially averaged SLA linear trend of 3.23 ± 0.61 mm/year from 1993 to 2019, which is not statistically different from the global average trend of 3.35 ± 0.4 mm/year estimated by Ablain et al. (2019) between 1993 and 2017. A widespread pattern of sea level rise was observed with strong positive and statistically significant trends over most of the region with maximum sea level rise obtained over the Mersa–Matruh and Cyprus gyres, as well as the North Shikmona eddy. In contrast a significant negative trend is observed over the Ierapetra gyre, whereas low and not statistically significant trends were only found in the southwestern part of the basin. The contributions of steric height and its components to total sea level rise in the EM were estimated for the period 1993–2019. The steric height of sea level rose at a rate of 1.38 ± 0.42 mm/year, accounting for 45% of the total sea level rise. This result is consistent with a global steric trend of 1.1 mm/year, which accounts for 44% of the total sea level rise from 1993 to 2017 (Storto et al., 2019). Also, this result is in agreement with Criado-Aldeanueva et al. (2008), who found that the steric effect accounts for 55% of total sea level trend in the Mediterranean Sea.

Thermosteric and halosteric components have opposing contributions to the sea level trend. The thermosteric effect, following the accelerating surface warming, is by far the main driver of sea level rise in EM over this period. The thermosteric component trend was 2.13 ± 0.41 mm/year, accounting for 69% of the total sea level trend. The halosteric trend was found to be negative in the largest part of the region, with a basin average of -0.75 ± 0.19 mm/year, con-

tributing (negatively) by 24% to the total sea level trend. These findings were in line with those obtained by [Storto et al. \(2019\)](#) for the North Atlantic Ocean. These authors demonstrated that the thermosteric effect dominates the steric sea level in the North Atlantic, while the halosteric component contributes negatively to the overall sea level trend. At the global scale, they found that about 25% of the temperature contribution to the total Steric SLA is compensated by salinity changes, in agreement with our result in the eastern Mediterranean.

The steric sea level in the eastern Mediterranean accounts for about 52% of total SLA interannual variability, which is consistent with [Storto et al. \(2019\)](#), who found that at the global scale, the steric sea level explains approximately 50%–70% of the sea level interannual variability. However, this is much higher than that observed by [Calafat et al. \(2012\)](#), who demonstrated that the steric effect explains less than 20% of the variance over the entire Mediterranean Sea and the eastern boundary of the North Atlantic northward of 45°N. They also found that the steric SLA in the eastern Mediterranean explains most of the sea level variation when compared to the western Mediterranean. The EM's dominance of the mass component is consistent with previous studies across the Mediterranean Sea ([Calafat et al., 2010](#)).

Over the study era, all tide gauges showed a positive and statistically significant trend. The most significant contributor to the SLA trend at the TG stations is again the thermosteric effect. However, at some stations, such as Thessaloniki, Leros, Antalya II, and Hadera the thermosteric contributions accounts for less than half of the observed trend, possibly due to the strong contribution of vertical land motion at these stations ([Fenoglio-Marc et al., 2004](#); [Mohamed and El-Din, 2019](#)), which is not addressed here. The interannual variability of SLA accounts for about 36% of overall sea level variability in the EM. On interannual time scales, atmospheric and steric effects contribute together ~70% to the total interannual variability of sea level from altimetry.

Our results demonstrate that increased warming is mainly responsible for the strong sea level rise in the Eastern Mediterranean Sea over the last two decades. Climate model projections indicate accelerating warming and sea level rise in the Mediterranean region during the twenty-first century ([Church et al. 2013](#)). Excessive sea level rise together with warming and drying of the Eastern Mediterranean basin are expected to have far-reaching environmental and societal impacts in this region.

Declaration of competing interest

The authors declare that they have no known competing financial interests or personal relationships that could have appeared to influence the work reported in this paper.

Acknowledgments

Authors would like to acknowledge the organizations that provided the sources of the data used in this work, including CMEMS Project for the altimetry and 3D temperature and

salinity products, the Permanent Service for Mean Sea Level (PSMSL) for tide gauge data, NOAA for the DOISST_V2.1 data, and AVISO for providing a comprehensive access to DAC data. The authors are also grateful to the anonymous reviewers, who have greatly improved the quality of this work with their advice and helpful remarks.

References

- Ablain, M., Meyssignac, B., Zawadzki, L., Jugier, R., Ribes, A., Spada, G., Benveniste, J., Cazenave, A., Picot, N., 2019. Uncertainty in satellite estimates of global mean sea-level changes, trend and acceleration. *Earth Syst. Sci. Data* 11, 1189–1202. <https://doi.org/10.5194/essd-11-1189-2019>
- Bonaduce, A., Pinaridi, N., Oddo, P., Spada, G., Larnicol, G., 2016. Sea-level variability in the Mediterranean Sea from altimetry and tide gauges. *Clim. Dyn.* 47, 2851–2866. <https://doi.org/10.1007/s00382-016-3001-2>
- Calafat, F.M., Chambers, D.P., Tsimplis, M.N., 2012. Mechanisms of decadal sea level variability in the eastern North Atlantic and the Mediterranean Sea. *J. Geophys. Res. Oceans* 117. <https://doi.org/10.1029/2012JC008285>
- Calafat, F.M., Marcos, M., Gomis, D., 2010. Mass contribution to Mediterranean Sea level variability for the period 1948–2000. *Glob. Planet. Change* 73, 193–201. <https://doi.org/10.1016/J.GLOPLACHA.2010.06.002>
- Carrère, L., Lyard, F., 2003. Modeling the barotropic response of the global ocean to atmospheric wind and pressure forcing – Comparisons with observations. *Geophys. Res. Lett.* 30. <https://doi.org/10.1029/2002GL016473>
- Cazenave, A., Bonnefond, P., Mercier, F., Dominh, K., Toumazou, V., 2002. Sea level variations in the Mediterranean Sea and Black Sea from satellite altimetry and tide gauges. *Glob. Planet. Change* 34, 59–86. [https://doi.org/10.1016/S0921-8181\(02\)00106-6](https://doi.org/10.1016/S0921-8181(02)00106-6)
- Cazenave, A., Cabanes, C., Dominh, K., Mangiarotti, S., 2001. Recent sea level change in the Mediterranean sea revealed by Topex/Poseidon satellite altimetry. *Geophys. Res. Lett.* 28, 1607–1610. <https://doi.org/10.1029/2000GL012628>
- Church, J., Clark, P., Cazenave, A., Gregory, J., Jevrejeva, S., Levermann, A., Merrifield, M., Milne, G., Nerem, R., Nunn, P., Payne, A., Pfeffer, W., Stammer, D., Unnikrishnan, A., 2013. Chapter 13: Sea Level Change. In: *Climate Change 2013: The Physical Science Basis: Contribution of Working Group I to the Fifth Assessment Report of the Intergovernmental Panel on Climate Change*. State Fed. Reports Publ.
- Criado-Aldeanueva, F., Del Río Vera, J., García-Lafuente, J., 2008. Steric and mass-induced Mediterranean sea level trends from 14 years of altimetry data. *Glob. Planet. Change* 60, 563–575. <https://doi.org/10.1016/J.GLOPLACHA.2007.07.003>
- Fenoglio-Marc, L., 2002. Long-term sea level change in the Mediterranean Sea from multi-satellite altimetry and tide gauges. *Phys. Chem. Earth* 27, 1419–1431. [https://doi.org/10.1016/S1474-7065\(02\)00084-0](https://doi.org/10.1016/S1474-7065(02)00084-0)
- Fenoglio-Marc, L., Dietz, C., Groten, E., 2004. Vertical land motion in the Mediterranean Sea from altimetry and tide gauge stations. *Mar. Geod.* 27, 683–701. <https://doi.org/10.1080/01490410490883441>
- Giorgi, F., 2006. Climate change hot-spots. *Geophys. Res. Lett.* 33. <https://doi.org/10.1029/2006GL025734>
- Gomis, D., Ruiz, S., Sotillo, M.G., Álvarez-Fanjul, E., Terradas, J., 2008. Low frequency Mediterranean sea level variability: The contribution of atmospheric pressure and wind. *Glob. Planet. Change* 63, 215–229. <https://doi.org/10.1016/j.gloplacha.2008.06.005>

- Greene, C.A., Thirumalai, K., Kearney, K.A., Delgado, J.M., Schwanghart, W., Wolfenbarger, N.S., Thyng, K.M., Gwyther, D.E., Gardner, A.S., Blankenship, D.D., 2019. The Climate Data Toolbox for MATLAB. *Geochem. Geophys. Geosy.* 20, 3774–3781. <https://doi.org/10.1029/2019GC008392>
- Guinehut, S., Dhomp, A.L., Larnicol, G., Le Traon, P.Y., 2012. High resolution 3-D temperature and salinity fields derived from in situ and satellite observations. *Ocean Sci.* 8, 845–857. <https://doi.org/10.5194/os-8-845-2012>
- Hamed, K.H., Ramachandra Rao, A., 1998. A modified Mann-Kendall trend test for autocorrelated data. *J. Hydrol.* 204, 182–196. [https://doi.org/10.1016/S0022-1694\(97\)00125-X](https://doi.org/10.1016/S0022-1694(97)00125-X)
- Huang, B., Liu, C., Banzon, V., Freeman, E., Graham, G., Hankins, B., Smith, T., Zhang, H.M., 2021. Improvements of the Daily Optimum Interpolation Sea Surface Temperature (DOISST) Version 2.1. *J. Clim.* 34, 2923–2939. <https://doi.org/10.1175/JCLI-D-20-0166.1>
- Hurrell, J.W., 1995. Decadal trends in the North Atlantic oscillation: Regional temperatures and precipitation. *Science* 269 (5224), 676–679. <https://doi.org/10.1126/SCIENCE.269.5224.676>
- Ibrahim, O., Mohamed, B., Nagy, H., 2021. Spatial Variability and Trends of Marine Heat Waves in the Eastern Mediterranean Sea over 39 Years. *J. Mar. Sci. Eng.* 9 (6), 643. <https://doi.org/10.3390/jmse9060643>
- Ishii, M., Kimoto, M., 2009. Reevaluation of historical ocean heat content variations with time-varying XBT and MBT depth bias corrections. *J. Oceanogr.* 65, 287–299. <https://doi.org/10.1007/s10872-009-0027-7>
- Jayne, S.R., Wahr, J.M., Bryan, F.O., 2003. Observing ocean heat content using satellite gravity and altimetry. *J. Geophys. Res. Ocean.* 108, 1–12. <https://doi.org/10.1029/2002jc001619>
- Jordà, G., Gomis, D., 2013. On the interpretation of the steric and mass components of sea level variability: The case of the Mediterranean basin. *J. Geophys. Res. Ocean.* 118, 953–963. <https://doi.org/10.1002/jgrc.20060>
- Landerer, F.W., Volkov, D.L., 2013. The anatomy of recent large sea level fluctuations in the Mediterranean Sea. *Geophys. Res. Lett.* 40, 553–557. <https://doi.org/10.1002/grl.50140>
- Levitus, S., Antonov, J.I., Boyer, T.P., Baranova, O.K., Garcia, H.E., Locarnini, R.A., Mishonov, A.V., Reagan, J.R., Seidov, D., Yarosh, E.S., Zweng, M.M., 2012. World ocean heat content and thermocline sea level change (0–2000m), 1955–2010. *Geophys. Res. Lett.* 39. <https://doi.org/10.1029/2012GL051106>
- Marcos, M., Tsimplis, M.N., 2008. Coastal sea level trends in Southern Europe. *Geophys. J. Int.* 175, 70–82. <https://doi.org/10.1111/j.1365-246X.2008.03892.x>
- McDougall, T.J., Barker, P.M., 2011. Getting started with TEOS-10 and the Gibbs Seawater (GSW) Oceanographic Toolbox. *Score/lapso Wg 127*, 28 pp.
- Menna, M., Gerin, R., Notarstefano, G., Mauri, E., Bussani, A., Paciaroni, M., Poulain, P.-M., 2021. On the Circulation and Thermohaline Properties of the Eastern Mediterranean Sea. *Front. Mar. Sci.* 8, art. 671469, 19 pp. <https://doi.org/10.3389/FMARS.2021.671469>
- Mohamed, B., Abdallah, A.M., Alam El-Din, K., Nagy, H., Shaltout, M., 2019a. Inter-Annual Variability and Trends of Sea Level and Sea Surface Temperature in the Mediterranean Sea over the Last 25 Years. *Pure Appl. Geophys.* 176, 3787–3810. <https://doi.org/10.1007/s00024-019-02156-w>
- Mohamed, B., El-Din, K.A., 2019. Sea level rise and vertical land motion in the eastern Mediterranean. In: 14th MEDCOAST Congress on Coastal and Marine Sciences, Engineering, Management and Conservation, MEDCOAST 2019, 479–486.
- Mohamed, B., Mohamed, A., Alam El-Din, K., Nagy, H., Elsherbiny, A., 2019b. Sea level changes and vertical land motion from altimetry and tide gauges in the Southern Levantine Basin. *J. Geodyn.* 128, 1–10. <https://doi.org/10.1016/J.JOG.2019.05.007>
- Nagy, H., Elgindy, A., Pinardi, N., Zavatarelli, M., Oddo, P., 2017. A nested pre-operational model for the Egyptian shelf zone: Model configuration and validation/calibration. *Dyn. Atmos. Ocean.* 80, 75–96. <https://doi.org/10.1016/j.dynatmoce.2017.10.003>
- Pascual, A., Marcos, M., Gomis, D., 2008. Comparing the sea level response to pressure and wind forcing of two barotropic models: Validation with tide gauge and altimetry data. *J. Geophys. Res. Ocean.* 113. <https://doi.org/10.1029/2007JC004459>
- Pastor, F., Valiente, J.A., Khodayar, S., 2020. A Warming Mediterranean: 38 Years of Increasing Sea Surface Temperature. *Remote Sens.* 12, 2687. <https://doi.org/10.3390/rs12172687>
- Pawlowicz, R., McDougall, T., Feistel, R., Tailleux, R., 2012. An historical perspective on the development of the Thermodynamic Equation of Seawater-2010. *Ocean Sci.* <https://doi.org/10.5194/os-8-161-2012>
- Peltier, W.R., Argus, D.F., Drummond, R., 2015. Space geodesy constrains ice age terminal deglaciation: The global ICE-6G-C (VM5a) model. *J. Geophys. Res. Solid Earth* 120, 450–487. <https://doi.org/10.1002/2014JB011176>
- Pujol, M.I., Larnicol, G., 2005. Mediterranean sea eddy kinetic energy variability from 11 years of altimetric data. *J. Mar. Syst.* 58, 121–142. <https://doi.org/10.1016/j.jmarsys.2005.07.005>
- Roether, W., Manca, B.B., Klein, B., Bregant, D., Georgopoulos, D., Beitzel, V., Kovačević, V., Luchetta, A., 1996. Recent changes in eastern Mediterranean deep waters. *Science* 271 (5247), 333–335. <https://doi.org/10.1126/SCIENCE.271.5247.333>
- Simav, M., Yıldız, H., Türkezer, A., Lenk, O., Özsoy, E., 2012. Sea level variability at Antalya and Menteş tide gauges in Turkey: Atmospheric, steric and land motion contributions. *Stud. Geophys. Geod.* 56, 215–230. <https://doi.org/10.1007/s11200-010-0067-x>
- Skliris, N., Sofianos, S., Gkanasos, A., Mantziafou, A., Vervatis, V., Axaopoulos, P., Lascaratos, A., 2012. Decadal scale variability of sea surface temperature in the Mediterranean Sea in relation to atmospheric variability. *Ocean Dyn.* 62, 13–30. <https://doi.org/10.1007/s10236-011-0493-5>
- Skliris, N., Zika, J.D., Herold, L., Josey, S.A., Marsh, R., 2018. Mediterranean sea water budget long-term trend inferred from salinity observations. *Clim. Dyn.* 51, 2857–2876. <https://doi.org/10.1007/S00382-017-4053-7>
- Stammer, D., Cazenave, A., Ponte, R.M., Tamisiea, M.E., 2013. Causes for Contemporary Regional Sea Level Changes. *Ann. Rev. Mar. Sci.* 5, 21–46. <https://doi.org/10.1146/annurev-marine-121211-172406>
- Stanev, E.V., Le Traon, P.Y., Peneva, E.L., 2000. Sea level variations and their dependency on meteorological and hydrological forcing: Analysis of altimeter and surface data for the Black Sea. *J. Geophys. Res. Ocean.* 105, 17203–17216. <https://doi.org/10.1029/1999jc900318>
- Storto, A., Bonaduce, A., Feng, X., Yang, C., 2019. Steric sea level changes from ocean reanalyses at global and regional scales. *Water (Switzerland)* 11, 1–31. <https://doi.org/10.3390/w11101987>
- Taibi, H., Haddad, M., 2019. Estimating trends of the Mediterranean Sea level changes from tide gauge and satellite altimetry data (1993–2015). *J. Oceanol. Limnol.* 37, 1176–1185. <https://doi.org/10.1007/s00343-019-8164-3>
- Torres, R.R., Tsimplis, M.N., 2013. Sea-level trends and interannual variability in the Caribbean Sea. *J. Geophys. Res. Ocean.* 118, 2934–2947. <https://doi.org/10.1002/jgrc.20229>
- Tsimplis, M.N., Álvarez-Fanjul, E., Gomis, D., Fenoglio-Marc, L., Pérez, B., 2005. Mediterranean Sea level trends: Atmospheric pressure and wind contribution. *Geophys. Res. Lett.* 32, 1–4. <https://doi.org/10.1029/2005GL023867>
- Tsimplis, M.N., Calafat, F.M., Marcos, M., Jordà, G., Gomis, D., Fenoglio-Marc, L., Struglia, M.V., Josey, S.A., Chambers, D.P.,

2013. The effect of the NAO on sea level and on mass changes in the Mediterranean Sea. *J. Geophys. Res. Ocean.* 118, 944–952. <https://doi.org/10.1002/jgrc.20078>
- Tsimplis, M.N., Josey, S.A., 2001. Forcing of the Mediterranean Sea by atmospheric oscillations over the North Atlantic. *Geophys. Res. Lett.* 28, 803–806. <https://doi.org/10.1029/2000GL012098>
- Tsimplis, M.N., Rixen, M., 2002. Sea level in the Mediterranean Sea: The contribution of temperature and salinity changes. *Geophys. Res. Lett.* 29. <https://doi.org/10.1029/2002GL015870>
- Vigo, I., Garcia, D., Chao, B.F., 2005. Change of sea level trend in the Mediterranean and Black seas. *J. Mar. Res.* 63, 1085–1100. <https://doi.org/10.1357/002224005775247607>
- Wang, G., Cheng, L., Boyer, T., Li, C., 2017. Halosteric sea level changes during the Argo era. *Water (Switzerland)* 9, 1–13. <https://doi.org/10.3390/w9070484>
- Wilks, D.S., 2011. *Statistical methods in the atmospheric sciences.* Academic Press.
- Woodworth, P.L., Player, R., 2003. The Permanent Service for Mean Sea Level: An Update to the 21st Century. *J. Coast. Res.* 19, 287–295.